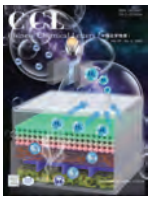
Chinese Chemical Letters 37 (2026) 111644

Contents lists available at ScienceDirect

Chinese Chemical Letters

journal homepage: www.elsevier.com/locate/cclet



Revealing the synergistic effect of materials composition and pollutants structure on catalytic degradation mechanism in heterogeneous iron-based Fenton-like reactions

Zhen Liu[a], Xinyi Xu[a], Jinkai He[a], Fei Xu[b], Qian Li[a,c,*]

[a] Shandong Key Laboratory of Water Pollution Control and Resource Reuse, Shandong Key Laboratory of Environmental Processes and Health, School of Environmental Science and Engineering, Shandong University, Qingdao 266200, China
[b] Environment Research Institute, Shandong University, Qingdao 266200, China
[c] Shenzhen Research Institute of Shandong University, Shenzhen 518057, China

ARTICLE INFO

Article history:
Received 18 December 2024
Revised 10 June 2025
Accepted 28 July 2025
Available online 5 August 2025

Keywords:
Fenton-like reaction
Electron transfer process
Graphitic nitrogen
Electron-donating organics
Selective degradation

ABSTRACT

Elucidating the synergistic influence mechanism of catalysts composition and pollutants structure on the treatment system is a necessary way to further expand the application potential of heterogeneous iron-based Fenton-like technology in the field of water treatment from catalytic source and degradation end. In this study, a nitrogen-doped iron-carbon material (Fe-NC-4%) was synthesized to effectively activate peroxymonosulfate (PMS) to remove different organic pollutants, thus further exploring the synergistic effects of material and pollutant structures on degradation performance and mechanism. A combination of characterization analysis, experimental demonstration and density functional theory calculation showed that the more graphitic nitrogen in Fe-NC-4% assisted the Fe active centers to adsorb PMS more easily and further form the Fe-NC-4%-PMS* complex with high activity and stability. And the Fe-NC-4%-PMS* complex could efficiently and selectively degraded electron-donating organics by electron transfer process (ETP). The degradation rate of ofloxacin (OFL) with stronger electron-donating ability could reach 0.405 min^{-1} in the Fe-NC-4%/PMS system. In addition, the Fe-NC-4%/PMS system possessed strong environmental adaptability, safety and practical application potential. This study would provide technical and theoretical guidance for the top-down analysis of specific reaction mechanisms in Fenton-like systems, including catalyst structure design, reactive species generation and selective pollutant degradation.

© 2026 Published by Elsevier B.V. on behalf of Chinese Chemical Society and Institute of Materia Medica, Chinese Academy of Medical Sciences.

As a highly efficient and promising water pollution control technology, the Fenton-like system has received much attention in the field of water environment improvement, especially in the removal of organic pollutants [1–5]. Among them, the protection and dispersion of activation sites by the materials structure as well as the efficient liquid-solid interfacial reaction ensure the high efficiency and stability of the heterogeneous catalytic system [6,7], thus making heterogeneous Fenton-like technology a better choice compared to other reaction systems. However, the low activation performance of heterogeneous catalysts, strong inhibition of reactive species by natural water factors, and complex contaminant structures are the common problems that hinder the application potential of heterogeneous Fenton-like technology [7,8]. Therefore, a large number of studies have chosen to introduce non-toxic Fe metal sites into heterogeneous catalysts to enhance the activation properties of materials, and combine their structural characteristics to further clarify the catalytic and degradation mechanisms [9]. Especially when the carbon material is used as the loading substrate, it could not only shorten the mass transfer distance between reactive substance and organics, but also optimize the adsorption performance of pollutants. Moreover, the high efficiency of electron conductivity also could contribute to the rapid generation of active species in the surface of carbon materials, and the contribution of non-radicals such as singlet oxygen is further amplified, which would also improve the environmental adaptability of the treatment system [10,11]. In addition, heteroatoms are often introduced into the carbon substrate to directly enhance the adsorption and catalytic performance of catalysts. For example, the introduction of nitrogen species is conducive to the fixation of Fe active sites, enhancing the stability of iron-based catalysts, and nitrogen atoms could further induce the generation of reactive species by regulating the overall electronic properties of the materials [11–14]. However, the diversity of material structures brings complexity to the

* Corresponding author.
E-mail address: qianli@sdu.edu.cn (Q. Li).

https://doi.org/10.1016/j.cclet.2025.111644
1001-8417/© 2026 Published by Elsevier B.V. on behalf of Chinese Chemical Society and Institute of Materia Medica, Chinese Academy of Medical Sciences.

study of catalytic mechanism. So, it is very important to improve the activity and stability of Fenton-like system from the perspective of catalysts design.

In addition to the catalyst structure, the diversity of organic pollutant structure also significantly affects the performance of the degradation system. Due to the different attack modes of electrophilic and nucleophilic reactive species on the active sites in organic matters, most of the current studies focus on the types and contributions of main reactive species in the degradation process of a target pollutant, but there is little discussion on the selective degradation of pollutants caused by different contributions of multiple active species in the reaction system. Some studies have begun to focus on and try to explain the degradation mechanism of pollutants from the perspective of reactive substances [15]. However, similar electrophilic attack properties make it difficult to distinguish the degradation contributions of traditional reactive oxygen species (ROS) in SR-AOPs, and the influence of catalyst composition on the production and reaction mechanisms of different active species (especially non-radical pathways in interfacial reactions) needs further investigation. Therefore, it is necessary to clarify the synergistic effects of catalyst structures, reactive species types and pollutant structures on catalytic and degradation mechanisms in heterogeneous Fenton-like systems.

In our previous study, we found that the developed nitrogen-doped iron-carbon catalyst (Fe-NC) formed by one-step carbonization using carboxymethyl chitosan (CMCs) hydrogel as template had good Fenton-like activity [16]. Therefore, in this study, this material was used to activate PMS to degrade different organic matters (taking norfloxacin (NOR) and ofloxacin (OFL) as the main target pollutants) to further explored and supplemented the catalytic degradation mechanism in the iron-based Fenton-like reaction. Specific discussions include: (1) Combining characterizations, experiments and theoretical calculations to clarify the influence of catalyst compositions on the activity, contribution and stability of the reactive species (especially the electron transport process); (2) The influence of pollutant structure on the adaptability and selectivity of the catalytic system was analyzed through the structural characteristics and degradation performance of different organics; (3) According to the synergistic influence analysis of catalyst compositions and pollutant structures, the environmental adaptability, safety and practical application potential of this degradation system were further proved.

The simple preparation process of Fe-NC-*x*% was shown in Fig. 1a. The X-ray diffraction (XRD) images showed that all catalysts had obvious characteristic peaks corresponding to Fe_3C, among which the characteristic peaks at 37.8°, 43.9° and 44.9° correspond to the (210), (102) and (031) crystal faces (JCPDS No. 85–1317), respectively (Fig. 1b). Some characteristic peaks could attribute to the Fe_3N structure also appear in different Fe-NC-*x*% (Fig. 1b). Scanning electron microscopy (SEM) images at different magnifications suggested that Fe-NC-4% was composed of loose porous carbon structure, and the carbon layer structure was embedded with dispersed small spherical iron nanoparticles (Figs. 1c and d). Transmission electron microscopy (TEM) images further indicated that the iron nanoparticles were encased in the outer "carbon shell" of Fe-NC-4%, with a typical graphite-carbon structure present in the carbon layer (Figs. 1e and f). And the TEM-mapping images showed that Fe nanoparticles were evenly dispersed in Fe-NC-4%, and a large number of C elements distributed in the same region as Fe elements further proved the dominant role of Fe_3C structure in the composition of material (Fig. 1g). In addition, X-ray photoelectron spectroscopy (XPS) analysis of different Fe-NC-*x*% suggested that different Fe species existed in Fe-NC-*x*%, which included Fe^{2+}(characteristic peaks at 710.22 eV (Fe^{2+} $2p_{3/2}$) and 723.69 eV (Fe^{2+} $2p_{1/2}$)), Fe^{3+} (714.29 eV (Fe^{3+} $2p_{3/2}$) and 728.09 eV (Fe^{3+} $2p_{1/2}$)) and Fe_2O_3 (719.21 eV) [17] (Fig. 1h). With the increase of carboxymethyl chitosan concentration, the Fe^{2+}/Fe^{3+} ratio of the material gradually decreased (Fig. S1 in Supporting information), and the high Fe^{2+} content of Fe-NC-4% might laid the foundation for its good Fenton-like catalytic performance. Moreover, according to the N 1s XPS spectrum, all three materials had four nitrogen species, and their characteristic peaks were centered on 397.31 eV (pyridinic N), 399.61 eV (pyrrolic N), 400.76 eV (graphitic N) and 404.80 eV (oxidized N), respectively (Fig. 1i) [18]. It is worth noting that the content of graphitic nitrogen and pyrrolic nitrogen in Fe-NC-*x*% gradually decreased with the increase of carboxymethyl chitosan concentration, while the content of pyridnic nitrogen gradually increased (Fig. 1j), which might directly affect the Fenton-like performance of the catalysts and lead to the change of pollutant degradation mechanism.

Two common quinolone antibiotics were selected as the primary target contaminants: Norfloxacin (NOR) and ofloxacin (OFL), with OFL having one additional -O- bond compared with NOR (Fig. 2a). The highest occupied and lowest unoccupied molecular orbitals (HOMO and LUMO) of NOR and OFL were calculated by density functional theory (DFT) calculation to further obtain their ionization potential (IP) values (Fig. S2 in Supporting information). The lower the IP value of organic matters, the stronger its electron-donating ability [19]. As shown in Figs. 2b and c and Fig. S2b, the degradation rates of OFL with lower IP value were higher than those of NOR in different Fe-NC-*x*%/PMS systems, and the catalytic performances of Fe-NC-4% in the degradation processes of NOR and OFL were higher than those of Fe-NC-6% and Fe-NC-8%. In addition, after determining the optimal basic conditions of the reaction system (catalysts dosage was 0.15 g/L, PMS concentration was 0.5 mmol/L) (Fig. S3 in Supporting information), the predominant role of Fe sites in the catalysts was further determined based on the shielding effect of SCN^- on Fe species [20]. As shown in Figs. 2d-f, the introduction of SCN^- significantly inhibited the degradation of pollutants in different reactions, especially SCN^- had a stronger inhibitory effect on the degradation performance of OFL (Fig. S4 in Supporting information). This not only indicated that the Fe sites were the main active sites on the surface of Fe-NC-*x*%, but also that the degradation of electron-donating contaminants (such as OFL) seemed to be more dependent on the good adsorption of HSO_5^- by Fe sites. In addition, compared with other reaction systems, 100 mmol/L SCN^- inhibited the degradation rates of NOR and OFL in the Fe-NC-4%/PMS system by up to 92.4% and 98.5% (Fig. 2f). Combined with XPS analysis, the Fe^{2+}/Fe^{3+} ratios in different catalysts were highly positively correlated with the degradation rate of NOR and OFL in different systems (Fig. S5 in Supporting information), and graphite nitrogen was more conducive to the degradation of organics than pyrrolic nitrogen and pyridinic nitrogen (Figs. 2g and h and Fig. S6 in Supporting information). Moreover, the Fe-NC-4%/PMS system had an obvious advantage over other reported systems in degrading NOR and OFL (Fig. 2i). Therefore, thanks to more active Fe(II) species and graphite nitrogen structure, the Fe-NC-4%/PMS system appeared to have stronger degradation efficiency for electron-donating organics. However, the specific reaction mechanism, including the influence of catalysts and pollutants structure on the catalytic degradation mechanism, needed further analysis.

The difference in the degradation performance of the Fe-NC-4%/PMS system for OFL and NOR might be attributed to the relative contribution of different reactive species produced in the activation reaction. First, methanol (MeOH), *tert*–butanol (TBA), *p*-benzoquinone (*p*-BQ) and L-histidine were selected as scavengers of $SO_4^{\bullet-}$, $^{\bullet}OH$, $^{\bullet}O_2^-$ and $^1O_2$, respectively, to elucidate the existence and species of reactive oxygen species (ROS) in the Fe-NC-4%/PMS system [21]. As shown in Figs. 3a-c, these four trapping agents

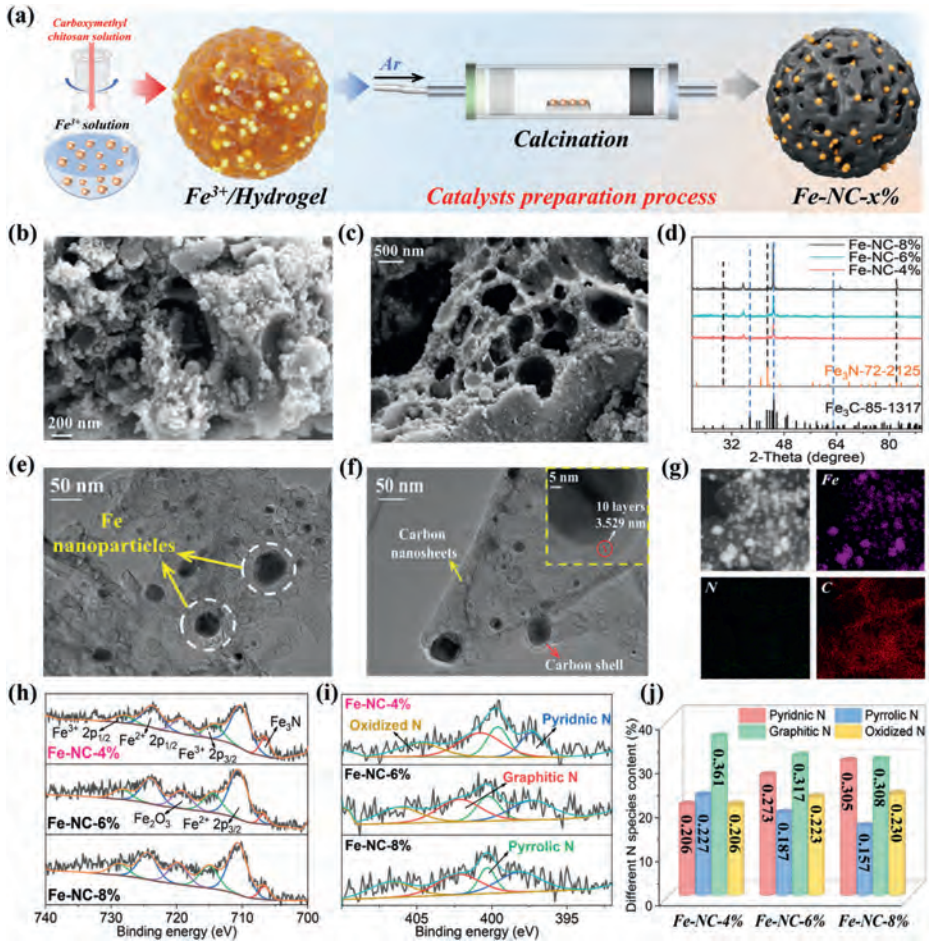


Fig. 1. (a) Preparation process of Fe-NC-*x*%. (b, c) SEM images with different magnifications of Fe-NC-4%. (d) XRD patterns of different Fe-NC-*x*% ($x = 4, 6, 8$). (e, f) TEM images of Fe-NC-4%. (g) TEM mapping of Fe-NC-4%. (h) Fe 2p XPS spectra of different Fe-NC-*x*% ($x = 4, 6, 8$). (i) N 1s XPS spectra of different Fe-NC-*x*% ($x = 4, 6, 8$). (j) Distribution of various N species of different Fe-NC-*x*% ($x = 4, 6, 8$).

obviously inhibited the degradation rates of pollutants, indicating that different reactive oxygen species were all involved in the removal of NOR and OFL. Moreover, MeOH and L-histidine showed stronger inhibitory effects on NOR and OFL degradation, respectively (Fig. 3c and Fig. S7 in Supporting information). According to the longer half-life of $^1O_2$ in D_2O, it was found that the Fe-NC-4%/PMS/D_2O system had stronger pollutant treatment performance than Fe-NC-4%/PMS/H_2O system (Fig. S8 in Supporting information). So, $SO_4^{\bullet-}$ and $^1O_2$ might be the dominant species for pollutant degradation. Furthermore, the types of ROS in the Fe-NC-4%/PMS system were determined by electron paramagnetic resonance (EPR) test. 5,5-Dimethyl-1-pyrroline *N*-oxide (DMPO) and 2,2,6,6-tetramethyl-4-piperidone (TEMP) were selected as the trapping agents of $SO_4^{\bullet-}$, $^{\bullet}OH$, $^{\bullet}O_2^-$ and $^1O_2$, respectively [22]. All four ROS signals were indeed present in the Fe-NC-4%/PMS system (Fig. 3d and Fig. S9 in Supporting information), but the introduction of NOR and OFL did not cause significant differences in the decline degree of reactive species' intensity (Fig. 3e and Fig. S9). Therefore, combined with the results of radical capture experiments, $^1O_2$ was not the main reason why OFL could be more efficiently degraded than NOR. In addition, the high-valenced iron species is also a non-radical path that could effectively degrade organic pollutants [23]. As could be seen in Fig. 3f, the conversion rate of PMSO to $PMSO_2$ $\eta(PMSO_2)$ in the Fe-NC-4%/PMS/PMSO system could reach 88.55%, but the concentration of PMSO only decreased by 15.7%, which indicated that there was not much Fe(IV) produced in the reaction. Although the $\eta(PMSO_2)$ was lower in the Fe-NC-4%/PMS/NOR (62.94%) and Fe-NC-4%/PMS/OFL (79.44%) systems (Fig. S10 in Supporting information), the introduction of PMSO did not significantly reduce the degradation of NOR or OFL in the Fe-NC-4%/PMS system (Figs. 3g and h). So, Fe(IV) was not the main active substance for the degradation of contaminants.

Electron-donating organics could be specifically degraded by electron transfer pathway (ETP) in heterogeneous Fenton-like reactions [24]. The simultaneous introduction of catalyst and PMS was used as the comparison group, the 5 min premixing experiments significantly inhibited NOR degradation (the degradation rate decreased from 0.399 min^{-1} to 0.077 min^{-1}) in the Fe-NC-4%/PMS system, but promoted the removal of OFL (the degradation rate increased from 0.071 min^{-1} to 0.151 min^{-1}) (Figs. 3i and j). This preliminarily suggested that ETP might be the dominant species in the rapid degradation of OFL. The electron transfer of OFL to the Fe-NC-4%/PMS system by salt bridge (5 μA) by galvanic oxidation process also directly confirmed the presence of ETP in the degradation system (Fig. S11 in Supporting information). *In-situ* Raman analysis also showed that an obvious characteristic peak (836 cm^{-1}) corresponding to the Fe-NC-4%-PMS* complex appeared on the surface of Fe-NC-4% after adsorption of PMS (Fig. 3k). This complex remained stable for 1–5 min (Fig. 3k), but after 10 min the Fe-NC-4%-PMS* complex might decompose into other active substances to further attack contaminants. Moreover, unlike NOR, the introduction of OFL caused the disappearance of the characteristic peak (836 cm^{-1}), which strongly proved the leading role of ETP in OFL degradation, and also indicated that ETP did not contribute

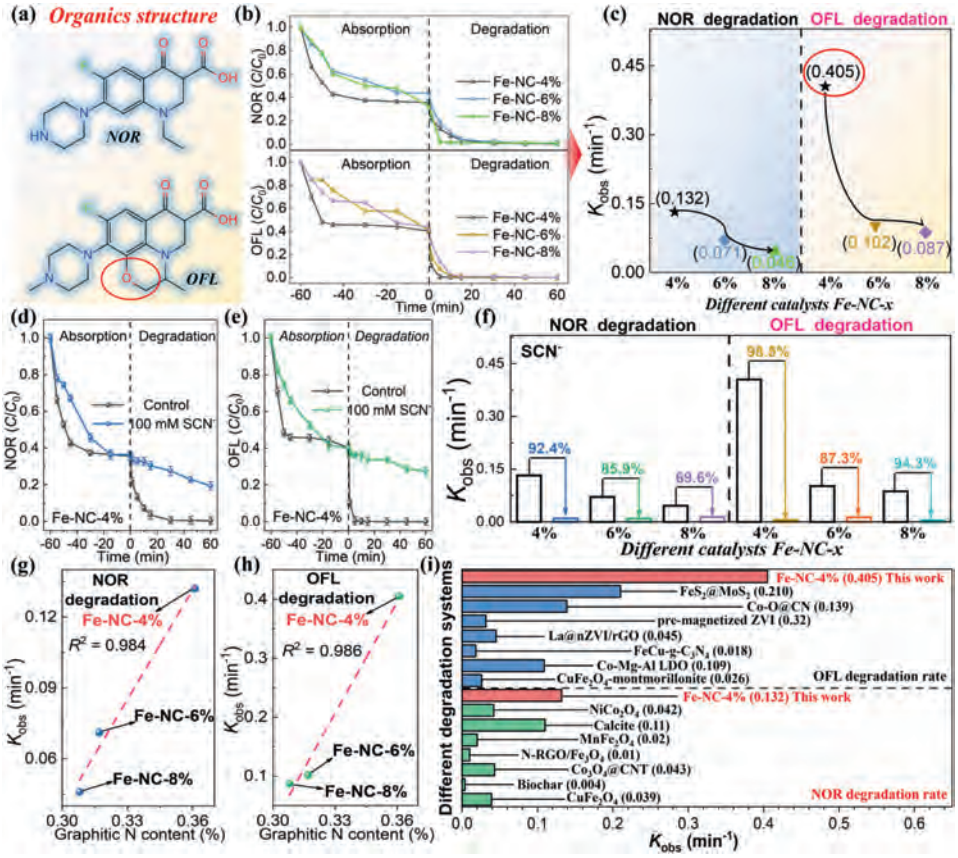


Fig. 2. (a) Structures of NOR and OFL. (b, c) The degradation performance of NOR and OFL in different Fe-NC-*x*%/PMS system. (d, e) The degradation performance of NOR and OFL in Fe-NC-4%/PMS/SCN^- system. (f) Effect on degradation rate of NOR and OFL in different Fe-NC-*x*%/PMS system by SCN^-. (g, h) Correlation analysis of graphitic nitrogen content and degradation rate of NOR or OFL. (i) Comparison of Fe-NC-4% with other reported work on degradation performance of NOR and OFL. Control condition: Catalysts dosage: 0.15 g/L; PMS concentration: 0.5 mmol/L; pH: 7.6; Temperature: 25 °C.

to NOR degradation. In addition, the higher degradation rate of OFL (0.862 min^{-1}) in the Fe-NC-4%/PMS/$NaClO_4$ system suggested that there was a strong inner sphere interaction between Fe-NC-4% and PMS (Fig. S12 in Supporting information) [25], which could further proved that the Fe-NC-4%-PMS* complex could stably and efficiently degrade contaminants *via* ETP. Therefore, the reactive species in Fe-NC-4%/PMS system could be divided into ROS, Fe(IV) and ETP. In order to further determine the influence of pollutants structure on the reaction mechanism, the competitive kinetics experiments were carried out with characteristic organic compounds (nitrobenzene (NB), benzoic acid (BA), *p*-BQ, furfuryl alcohol (FFA)) and pollutants (OFL or NOR), and the relative contribution rates of different reactive species in the degradation reactions were studied in detail. According to the second-order rate constants of OFL and NOR reacting with different ROS obtained in the competitive experiments (Figs. S13-S16 in Supporting information) (Text S6 in Supporting inofrmation), it was calculated that the steady-state concentrations of ROS in the Fe-NC-4%/PMS/NOR system were higher than those in the Fe-NC-4%/PMS/OFL system (Fig. 3l). The resulting relative degradation contribution rates showed that $SO_4^{\bullet-}$ played a leading role in the Fe-NC-4%/PMS/NOR system (65%), while Fe(IV)+ETP dominated the degradation of OFL (Fig. 3m and Figs. S17-S19 in Supporting information). However, the influence of PMSO had shown that Fe(IV) was not the main species of OFL degradation, so ETP dominated the removal of OFL. In short, the degradation mechanism of the same Fenton-like system was easily affected by the structure of pollutants.

In addition to the structure of pollutants, the different composition of catalysts is also a key factor affecting the heterogeneous surface activation mechanism and the intensity of the corresponding reactive species. The activation properties of different catalysts showed that, in addition to the Fe active center, the graphitic nitrogen structure was also important for improving the catalytic activity of materials. Therefore, the Fe-NC-8% with the least graphitic nitrogen content was selected as the control group to further elucidate the influence of material structure on the activation mechanism. Compared with the Fe-NC-4%/PMS system (Figs. 3a-c), different trapping agents could inhibit NOR and OFL degradation in the Fe-NC-8%/PMS system (Figs. 4a-c). Especially in the Fe-NC-8%/PMS/MeOH system, the degradation rates of NOR and OFL decreased from 0.046 to 0.087 min^{-1} to 0.017 and 0.015 min^{-1}, respectively. This intuitively suggested that $SO_4^{\bullet-}$ might be the dominant species in the Fe-NC-8%/PMS system. In addition, the PMSO conversion rate ($\eta(PMSO_2)$, 82.17%) in the Fe-NC-8%/PMS system was smaller than that in the Fe-NC-4%/PMS system (Fig. 4d), which might be due to the fact that more graphite-nitrogen species enhanced the reactivity of the Fe activation center by promoting electron transport [26]. In addition, although PMSO did not significantly inhibit the degradation of OFL (11.5%) and NOR (34.8%) in Fe-NC-8%/PMS system (Figs. 4e and f), the corresponding inhibitory effect was greater than that in Fe-NC-4%/PMS system (Figs. 3g and h). Therefore, more graphite-nitrogen structure facilitated the production of Fe(IV), but weakened its contribution in the degradation reactions. According to the steady-state concentration of ROS and the relative contribution rates of different reactive species in the Fe-NC-8%/PMS system (Figs. 4g, h and Figs. S20-S22 in Supporting information), $SO_4^{\bullet-}$ was the dominant species in NOR (75.22%) and OFL (81.53%) degradation in the Fe-NC-8%/PMS

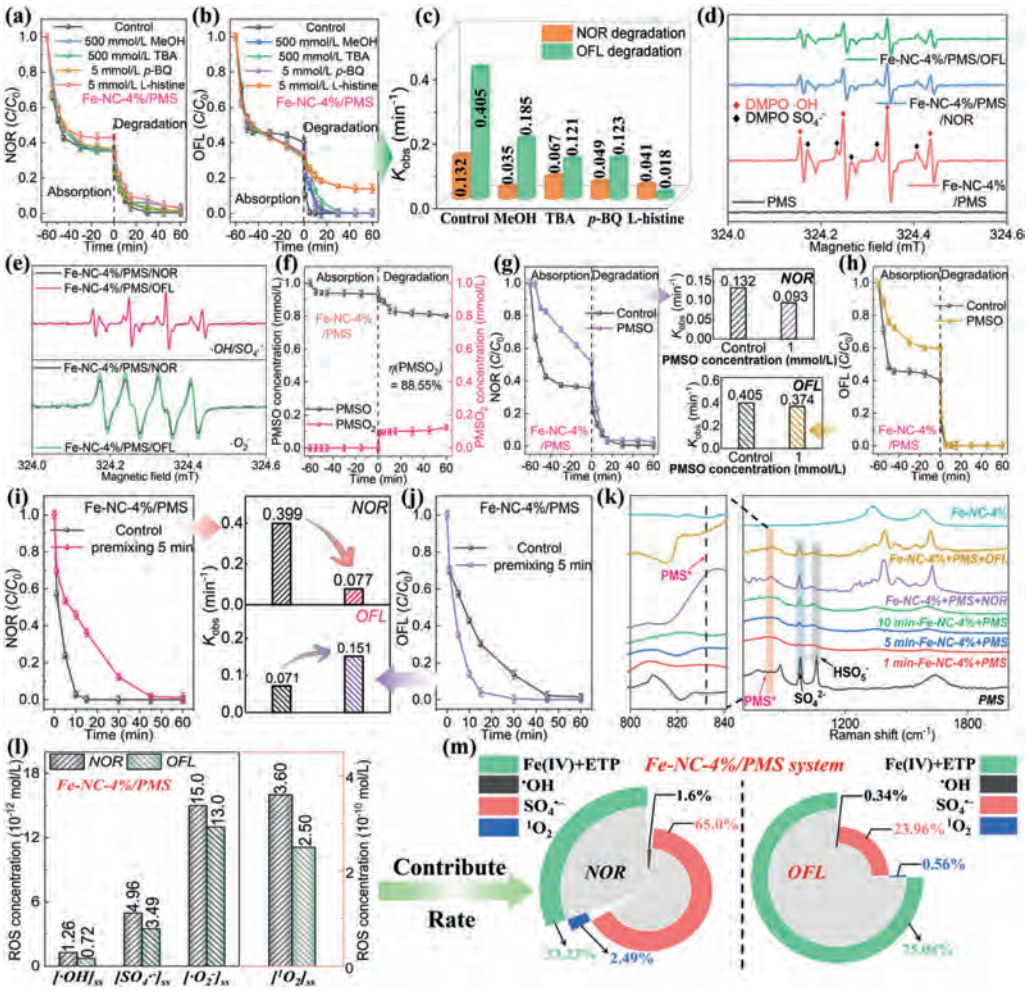


Fig. 3. (a-c) Quenching experiments in the Fe-NC-4 %/PMS/NOR and Fe-NC-4 %/PMS/OFL systems. (d) EPR analysis of $SO_4^{\bullet-}$ and $^{\bullet}OH$ signals in the different reaction systems. (e) Effect of NOR and OFL on ROS signals in the Fe-NC-4 %/PMS system. (f) Degradation of PMSO and transformation of $PMSO_2$ in the Fe-NC-4 %/PMS system. (g, h) Effect of PMSO on NOR and OFL degradation in the Fe-NC-4 %/PMS system. (i, j) Effect of premixing experiment on degradation of NOR and OFL in Fe-NC-4 %/PMS system. (k) *In-situ* Raman analysis. (l) The steady-state concentrations of ROS in Fe-NC-4 %/PMS system. (m) The relative contribution rates of different ROS during NOR and OFL degradation in Fe-NC-4 %/PMS system. Control condition: Catalysts dosage: 0.15 g/L; PMS concentration: 0.5 mmol/L; pH: 7.6; Temperature: 25 °C.

system, rather than ETP. Compared with the Fe-NC-4 %/PMS system, the difference in the contribution rate of ETP to OFL degradation directly indicated that more graphitic nitrogen structures contributed to higher ETP activity in heterogeneous interfacial reaction system.

According to the characterization results of different materials, density functional theory (DFT) calculations were used to further investigate the effect of material structure on the catalytic reaction. Two materials, Fe-NC-4 % and Fe-NC-8 %, with the largest difference in graphitic nitrogen content, were selected to construct the comparison models (Fig. 4i and Fig. S23 in Supporting information). It could be seen from Figs. 4i and j that the PMS adsorption energy of Fe-NC-4 % (−8.972 eV) was higher than that of Fe-NC-8 % (−3.278 eV). This would facilitate the generation of catalysts-PMS* complexes in interfacial activation reactions of Fe-NC-4 %/PMS system and laid the foundation for the production of ETP and subsequent other reactive species (such as ROS). In addition, the cleavage of O–O and O–H bonds during the heterogeneous PMS activation is directly responsible for the generation of ROS in interfacial catalytic reactions (Fig. S24 in Supporting information) [27]. The O–O and O–H bond lengths of PMS adsorbed on the surface of Fe-NC-4 % (1.498 and 0.996 Å) were longer than those of the Fe-NC-8 %/PMS system (1.492 and 0.986 Å) (Fig. 4j), which suggested that Fe-NC-4 % was more likely to activate PMS to produce ROS than Fe-NC-8 %. And the charge difference between the two reaction systems showed that Fe-NC-4 % (0.84 e) transferred more electrons to PMS than Fe-NC-8 % (0.80 e) (Figs. 4k, l and Fig. S25 in Supporting information), which also explained the stronger activation performance of Fe-NC-4 %. Therefore, the special reaction mechanism of the Fe-NC-4 %/PMS system was that with the help of graphitic nitrogen structure, the Fe active center on the surface of the materials first adsorbed PMS to form the Fe-NC-4 %-PMS* complex, and this complex could directly and rapidly degrade OFL *via* ETP (Fig. 4m). Then the rapid electron transfer between Fe-NC-4 % and PMS accelerated the O–O bond breaking in the adsorbed PMS to form $SO_4^{\bullet-}$, which then reacted with water molecules to produce $^{\bullet}OH$ (Fig. S26 in Supporting information). And through a series of reactions between HSO_5^- and water molecules could form $^{\bullet}O_2^-$ and $^1O_2$ (Fig. S26). Finally, different ROS produced in the Fe-NC-4 %/PMS system were used for NOR or OFL removal. In conclusion, more active structures in Fe-NC-4 % were the fundamental reason for the efficient generation of reactive species, and the different structures of pollutants further mediate the change of the relative contributions of different active substances, and finally cooperate to achieve selective degradation of Fenton-like system.

By further analyzing the removal mechanism of various organics in different degradation systems, the synergistic mechanism of material structure and pollutant characteristics in Fenton-like reac-

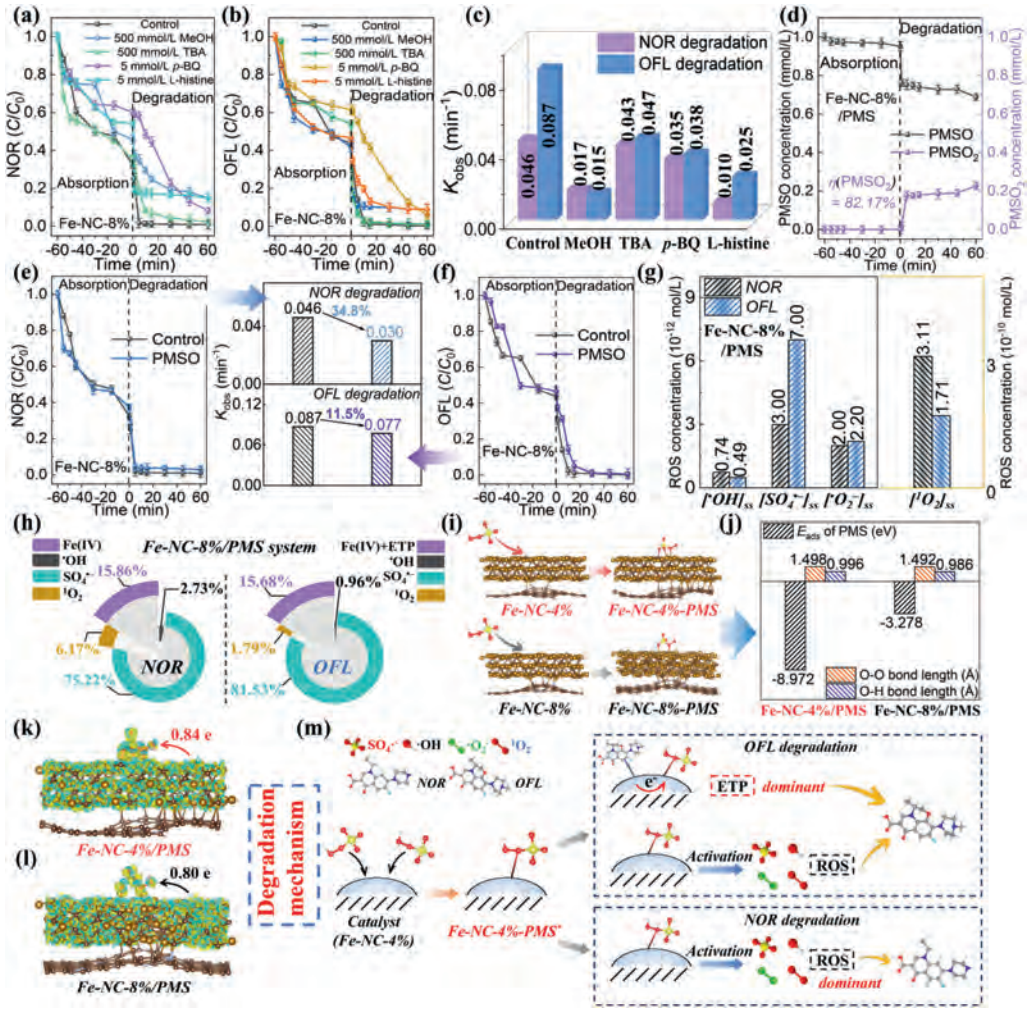


Fig. 4. (a-c) Quenching experiments in the Fe-NC-8 %/PMS/NOR and Fe-NC-8 %/PMS/OFL systems. (d) Degradation of PMSO and transformation of $PMSO_2$ in the Fe-NC-8 %/PMS system. (e, f) Effect of PMSO on NOR and OFL degradation in the Fe-NC-8 %/PMS system. (g) The steady-state concentrations of ROS in Fe-NC-8 %/PMS system. (h) The relative contribution rates of different ROS during NOR and OFL degradation in Fe-NC-8 %/PMS system. (i) The adsorption of PMS by Fe-NC-4 % and Fe-NC-8 %. (j) The adsorption energy of PMS, O–O and O–H bond length in Fe-NC-4 %/PMS and Fe-NC-8 %/PMS systems. (k, l) Charge transfer to PMS in different systems. (m) Degradation mechanism of NOR and OFL in Fe-NC-4 %/PMS system. Control condition: Catalysts dosage: 0.15 g/L; PMS concentration: 0.5 mmol/L; pH: 7.6; Temperature: 25 °C.

tion was clarified. According to the different characteristics of the groups in the organic molecules, the pollutants could be roughly divided into three types: electron-donating organics, electron-absorbing organics and mixed organics (Fig. 5a). And the IP values of electron-donating organics are generally lower than those of electron-absorbing organics, and this difference would affect the degradation characteristics of pollutants in Fenton-like reactions, and even lead to selective degradation. So, seven special organics including nitrobenzene (NB), benzoic acid (BA), p-hydroxybenzoic acid (*p*-HBA), *p*-nitrobenzoic acid (*p*-NBA), 4-nitrophenol (4-NP), aniline (AL) and phenol (PE) were selected to collaborate with NOR and OFL to validate the selectivity of the Fe-NC-4 %/PMS system. As shown in Figs. 5b and c, the HOMO and LUMO values of different organics were calculated by DFT analysis, and their IP values were further obtained (Fig. S27 in Supporting information). According to IP value, OFL had stronger electron donating ability, and organics containing amino and hydroxyl groups were more likely to give electrons than pollutants with carboxyl and nitro structures (Fig. S27). The Fukui index further showed that the benzene ring and electron-donating groups in the seven organics such as AL were more vulnerable to electrophilic attack by reactive species, and the low electron cloud on the electron-absorbing groups (carboxyl and nitro groups) might lead to a decrease in the overall degradation efficiency of organic molecules. As shown in Figs. 5d and e, the degradation performances of electron-donating organics were higher than those of electron-absorbing pollutants and mixed pollutants. In the Fe-NC-4 %/PMS system, the degradation rates of aniline and phenol could reach 0.216 min^{-1} and 0.075 min^{-1}, while the degradation rates of NB and *p*-NBA were as low as 0.003 min^{-1} and 0.008 min^{-1} (Fig. 5e). And the similar degradation rules also appeared in the Fe-NC-8 %/PMS system, but the degradation rates of different organics were lower than those of the Fe-NC-4 %/PMS system (Fig. 5d). Interestingly, the degradation rates of aniline and phenol in the Fe-NC-8 %/PMS system were only 0.077 min^{-1} and 0.032 min^{-1}, but the degradation rates of NB and p-NBA with larger IP values were maintained at 0.002 min^{-1} and 0.008 min^{-1} (Fig. 5e). Combined with the effect of graphitic nitrogen content on the degradation rates of different organics (Fig. S28 in Supporting information), more Fe active sites and graphitic nitrogen structure made the Fe-NC-4 %-PMS* complex possess better degradation performance for electron-donating pollutants than the Fe-NC-8 %-PMS* complex. In addition, there was a good negative correlation between the degradation rates of organics and IP values in different reaction systems (Figs. 5f and g). Therefore, pollutant structure and material structure synergistically affect the selective degradation performance of Fenton-like system, and the

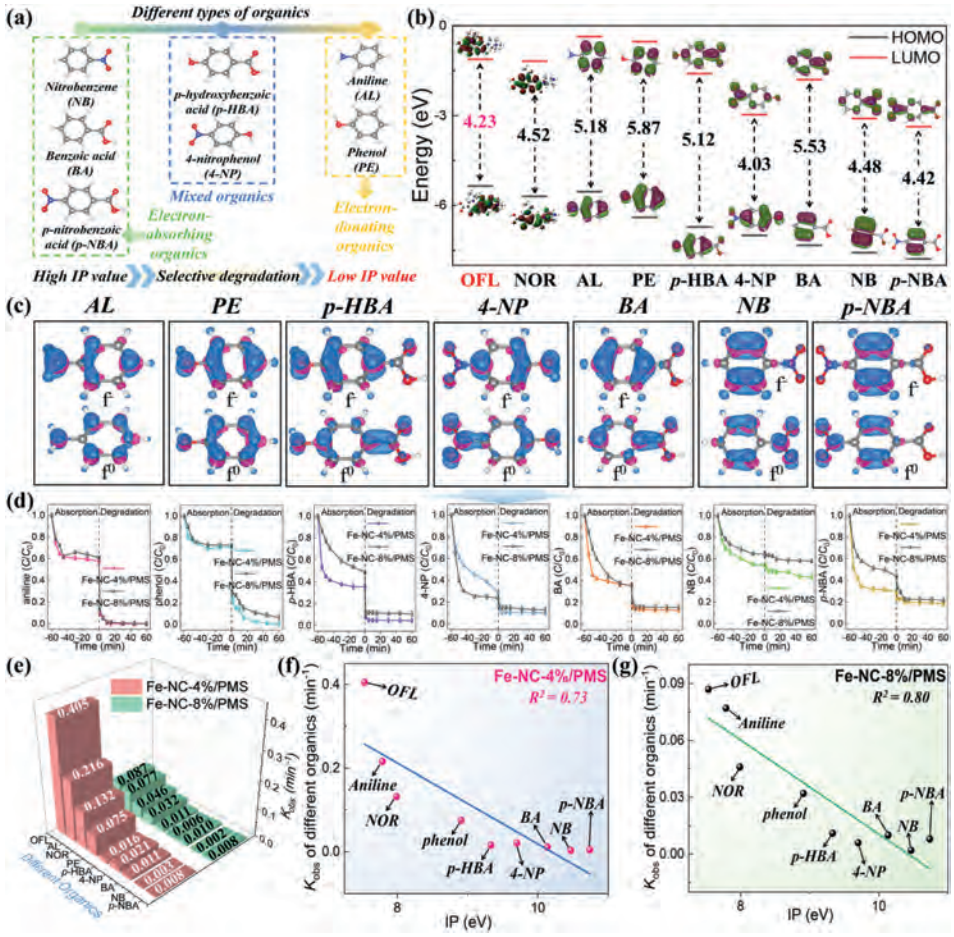


Fig. 5. (a) Structure and characteristics of different types of pollutants. (b) HOMO and LUMO of different organics. (c) Fukui index of different organics. (d) Degradation performance of different organics in the Fe-NC-4%/PMS and Fe-NC-8%/PMS systems. (e) Degradation rates of different organics in the Fe-NC-4%/PMS and Fe-NC-8%/PMS systems. (f) Relationship between degradation rates and IP values of different pollutants in the Fe-NC-4%/PMS system. (g) Relationship between degradation rates and IP values of different pollutants in the Fe-NC-8%/PMS system.

Fe-NC-4%/PMS system could selectively degrade electron-donating pollutants.

Experiments on the effects of different pH values, inorganic anions and humic acids further suggested that the Fe-NC-4%/PMS system possessed good environmental adaptability (Figs. S29-S31 in Supporting information). And, in different water matrices (*e.g.*, tap water (TW), river water (RW), secondary treated water (STW) and seawater (SW)), the Fe-NC-4%/PMS system could also effectively degrade organic pollutants (Fig. S32 in Supporting information). In addition, the Fe-NC-4%/PMS system still maintained 88.6% of degradation efficiency after five cycles (Fig. S29f). In particular, the Fe-NC-4%/PMS system could degrade 95.8% NOR and 100% OFL after 8 cycles by the fluidity experiment device (Figs. S29g-i). As shown in Fig. S33 (Supporting information), Fe-NC-4% still maintained a good basic crystal structure after the reaction. Combined with the small leaching amount of Fe ion in the reaction (Fig. S34 in Supporting information), it could be seen that the Fe-NC-4%/PMS system had good practical application potential and environmental safety. Combined with the DFT calculation and high performance liquid chromatography and mass spectrometry (HPLC-MS) analysis (Figs. S35 and S37 in Supporting information), the degradation process of NOR in Fe-NC-4%/PMS system could be roughly divided into four main ways: piperazine ring opening, defluorination, decarboxylation, and hydroxylation. And the results of HPLC-MS analysis further identified eight possible degradation pathways of OFL, including decarboxylation, hydroxylation, methyl substitution, piperazine ring opening, piperazine dealkylation, and cleavage (Figs. S36 and S37 in Supporting information). Therefore, the change of pollutant structure made the degradation process of OFL more complex and diverse than NOR. According to the degradation paths of NOR and OFL, the environmental safety of the Fe-NC-4%/PMS system was evaluated by the quantitative structure-activity relationship (QSAR) using two representative indicators of acute toxicity and bioaccumulation factors (Text S11 in Supporting information). As shown in Figs. S35e-h, acute toxicity of most products in the degradation processes of NOR and OFL was significantly reduced, while toxicity of a few intermediates increased, but decreased after further degradation. In particular, piperazine ring-opening products (such as D2, D3, P9 and P10) had lower biotoxicity. The change trend of bioaccumulation factors was similar to that of acute toxicity, and some intermediates with higher toxicity were further transformed into less toxic products. In addition, after treatment with the Fe-NC-4%/PMS system, the TOC values of different water bodies containing NOR and OFL decreased significantly (Fig. S38 in Supporting information). Although different water matrixes affected the treatment performance of the reaction system, the existence of efficient degradation pathways such as ETP ensured that the Fe-NC-4%/PMS system had better wastewater treatment performance and environmental safety. Therefore, the Fe-NC-4%/PMS system helped

to reduce the biological toxicity of organic pollutants in water ecosystems.

In this study, the nitrogen-doped iron-carbon material Fe-NC-4% was used to efficiently activate PMS to degrade organic pollutants, and then the synergistic mechanism of material composition and pollutant structure affecting Fenton-like properties was expounded. Compared with NOR (0.132 min^{-1}), the Fe-NC-4%/PMS system had better degradation performance for electron-donating organic OFL (0.405 min^{-1}). And in the Fe-NC-4%/PMS system, $SO_4^{\bullet-}$ and ETP were the dominant reactive species for NOR and OFL degradation, respectively. Combined with the characterization, experimental analysis and DFT calculation results, more graphitic nitrogen structure helped Fe active sites to enhance the adsorption performance of PMS (−8.972 eV), thus forming a strong and stable Fe-NC-4%-PMS* complex. And the Fe-NC-4%-PMS* complex could efficiently and selectively degrading electron-donating organics through ETP. In addition, the influence of environmental factors such as inorganic anions directly proved the stability and adaptability of non-radical pathway ETP in water treatment. Finally, the Fe-NC-4%/PMS system further showed strong environmental adaptability, safety and recycling. This study would provide theoretical and technical support for catalyst design and selective degradation of pollutants in Fenton-like systems, and helped further elucidation of the origin and mechanism of reactive species in advanced oxidation technologies.

Declaration of competing interest

The authors declare that they have no known competing financial interests or personal relationships that could have appeared to influence the work reported in this paper.

CRediT authorship contribution statement

Zhen Liu: Writing – original draft, Investigation, Formal analysis, Data curation. **Xinyi Xu:** Formal analysis. **Jinkai He:** Data curation. **Fei Xu:** Writing – review & editing. **Qian Li:** Writing – review & editing, Funding acquisition.

Acknowledgments

This work was supported by the National Natural Science Foundation of China (Nos. 52070121 and U22A20423). This study was also supported by the Taishan Scholars Foundation of Shandong Province (No. tsqn202312039) and Shenzhen Fundamental Research Program (JCYJ20240813101101002). Thanks to the Analytical Testing Center of School of Environmental Science and Engineering of Shandong University and the State Key Laboratory of Microbiology Technology of Shandong University for the equipment support.

Supplementary materials

Supplementary material associated with this article can be found, in the online version, at doi:10.1016/j.cclet.2025.111644.

References

[1] Z. Zhao, H. Tan, P. Zhang, et al., Angew. Chem. Int. Ed. 62 (2023) e202219178.
[2] J. Hu, H. Gong, K. Fu, J. Jia, N. Zhu, et al., Water Res. 261 (2024) 122020.
[3] C. Zhang, N. Ding, Y. Pan, et al., Chin. Chem. Lett. 35 (2024) 109579.
[4] Y. Jiang, Z. Yang, X. Bi, et al., Chin. Chem. Lett. 35 (2024) 109331.
[5] W. Zhu, W. Zuo, P. Wang, et al., Chin. Chem. Lett. 34 (2024) 109341.
[6] S. Wang, S. Gao, J. Tian, et al., J. Hazard. Mater. 387 (2020) 121995.
[7] M. Hu, J. Zhu, W. Zhou, et al., Environ. Pollut. 270 (2021) 116092.
[8] D. Li, X. Zhang, Y. Sun, et al., J. Hazard. Mater. 465 (2024) 133425.
[9] F.S. Mustafa, K.H. Hama Aziz, Process Saf. Environ. Prot. 170 (2023) 436–448.
[10] K.H. Hama Aziz, RSC Adv. 13 (2023) 115–128.
[11] Y.X. Huang, K.Y. Chen, S.X. Wang, et al., Appl. Catal. B 341 (2024) 123324.
[12] W. Xiao, A. Chen, M. Cheng, et al., Water Res. 268 (2025) 122735.
[13] A. Chen, M. Cheng, G. Wang, et al., Sep. Purif. Technol. 354 (2025) 129432.
[14] H. Liu, M. Cheng, Y. Liu, et al., Sep. Purif. Technol. 355 (2025) 129659.
[15] Z. Chen, X. Wang, M. Zhang, et al., J. Colloid Interface Sci. 670 (2024) 323–336.
[16] J. He, J. Huang, Z. Wang, et al., Chem. Eng. J. 439 (2022) 135784.
[17] Y. Sun, Y. Wang, H. Ma, et al., Carbon 178 (2021) 515–527.
[18] W. Liu, L. Zhang, X. Liu, et al., J. Am. Chem. Soc. 139 (2017) 10790–10798.
[19] W. Cao, W. Chen, S. Sun, et al., J. Mol. Struct.: THEOCHEM 817 (2007) 1–4.
[20] J. Hu, S. Wang, J. Yu, et al., Environ. Sci. Technol. 55 (2021) 1260–1269.
[21] Z. Liu, S. Pan, F. Xu, et al., Water Res. 225 (2022) 119142.
[22] Z. Liu, R. Su, X. Sun, et al., Sci. Total Environ. 741 (2020) 140464.
[23] Q. Yan, C. Lian, K. Huang, et al., Angew. Chem. Int. Ed. 60 (2021) 17155–17163.
[24] W. Ren, C. Cheng, P. Shao, et al., Environ. Sci. Technol. 56 (2022) 78–97.
[25] Y. Ding, X. Wang, L. Fu, et al., Sci. Total Environ. 765 (2021) 142794.
[26] Z. Liu, R. Su, F. Xu, et al., Adv. Mater. 36 (2024) 202311869.
[27] Z. Liu, Y. Hu, Y. Huang, Sep. Purif. Technol. 342 (2024) 127077.